Universiteit
Leiden
The Netherlands

Shear stress regulated signaling in renal epithelial cells and polycystic kidney disease

Kunnen, S.J.

Citation
Kunnen, S. J. (2018, September 27). *Shear stress regulated signaling in renal epithelial cells and polycystic kidney disease*. Retrieved from https://hdl.handle.net/1887/66002

Version:	Not Applicable (or Unknown)
License:	Licence agreement concerning inclusion of doctoral thesis in the Institutional Repository of the University of Leiden
Downloaded from:	https://hdl.handle.net/1887/66002

Note: To cite this publication please use the final published version (if applicable).

Cover Page

Universiteit Leiden

The handle http://hdl.handle.net/1887/66002 holds various files of this Leiden University dissertation.

Author: Kunnen, S.J.
Title: Shear stress regulated signaling in renal epithelial cells and polycystic kidney disease
Issue Date: 2018-09-27

CHAPTER 5

Inhibition of Activin signaling slows progression of Polycystic Kidney Disease in mice.

Wouter N. Leonhard[1], Steven J. Kunnen[1], Anna J. Plugge[1], Arja Pasternack[4], Sebastian B.T. Jianu[1], Kimberley Veraar[2], Fatiha el Bouazzaoui[1], Willem M.H. Hoogaars[5], Peter ten Dijke[3], Martijn H. Breuning[1], Emile De Heer[2], Olli Ritvos[4], Dorien J.M. Peters[1].

[1]Dept. of Human Genetics, [2]Pathology and [3]Molecular Cell Biology and Cancer Genomics Centre Netherlands at the Leiden University Medical Center. [4]Dept of Bacteriology and Immunology, Haartman Institute, University of Helsinki, Finland. [5]Department of Human Movement Sciences, Faculty of Behavior and Movement Sciences, Vrije Universiteit Amsterdam, MOVE Research Institute Amsterdam, The Netherlands.

J Am Soc Nephrol. 2016; 27(12): 3589-3599

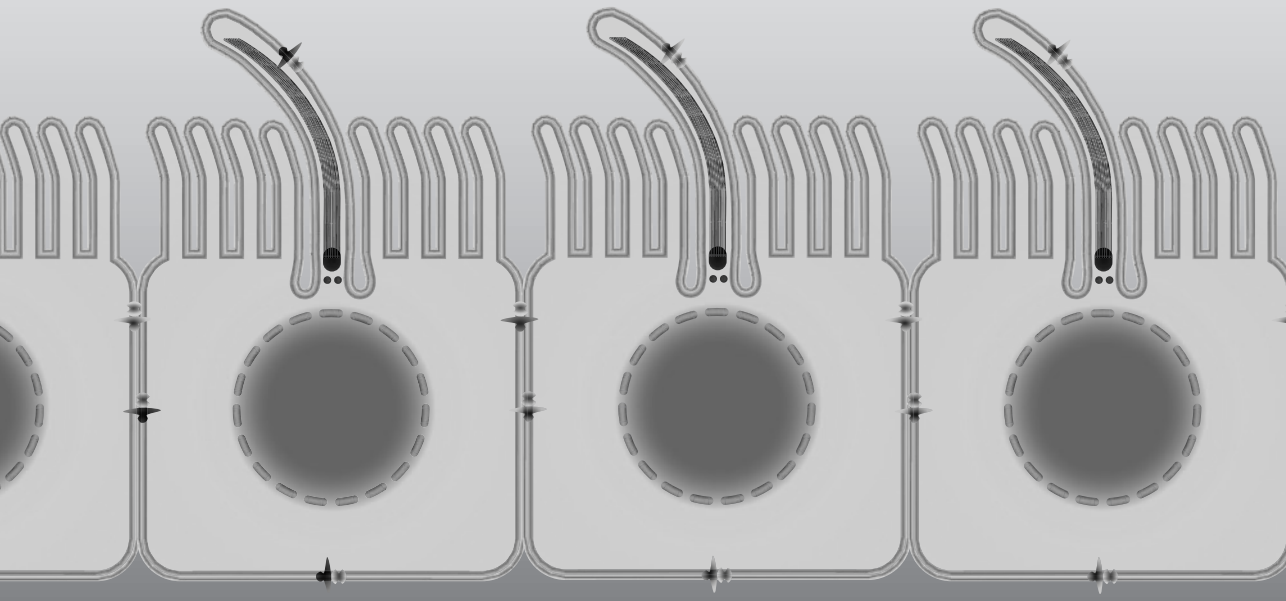

ABSTRACT

Autosomal Dominant Polycystic Kidney Disease (ADPKD), characterized by the formation of numerous kidney cysts, is caused by *PKD1* or *PKD2* mutations and affects 0.1% of the population. Although recent clinical studies indicate that reduction of cAMP levels slows progression of PKD, they have not yet led to an established safe and effective therapy for patients, indicating the need to find new therapeutic targets. The role of transforming growth factor β (TGFβ) in PKD is not clearly understood but nuclear accumulation of pSMAD2/3 in cyst-lining cells suggests the involvement of TGFβ signaling in PKD. In this study we ablated the TGFβ type I receptor (also termed activing receptor-like kinase 5 (ALK5)) in renal epithelial cells of PKD mice, which had little to no effect on the expression of SMAD2/3 target genes, or on the progression of PKD. These data suggest that alternative TGFβ superfamily ligands may account for SMAD2/3 activation in cystic epithelial cells. Activins are members of the TGFβ superfamily and drive SMAD2/3 phosphorylation via Activin receptors and have not yet been studied before in the context of PKD. Already in mice with early PKD, we found increased expression of Activin ligands. In addition, treatment with a soluble Activin receptor IIB fusion protein (sActRIIB-Fc), which acts as a soluble trap to sequester Activin ligands, effectively inhibited cyst formation in three distinct mouse models of PKD. These data point to Activin signaling as a key player in PKD, and as a promising target for therapy.

INTRODUCTION

Autosomal Dominant Polycystic Kidney Disease (ADPKD) is a frequent disorder affecting 1 in 1000 individuals and involves the *polycystic kidney disease 1 (PKD1)* gene, which is mutated in 85% of the cases, and the *PKD2* gene, which is mutated in 15% of the cases[1-3]. Besides extra-renal manifestations such as liver cysts, pancreas cysts, hypertension, cardiovalvular abnormalities and cerebral aneurisms, the kidney is the most severely affected organ[4]. Patients develop thousands of renal cysts causing anatomically distorted, enlarged and fibrotic kidneys, which ultimately leads to renal failure around the age of 60 years[5,6]. When the levels of functional Polycystin 1 (PC1) or Polycystin 2 (PC2), the gene-products of *PKD1* and *PKD2*, deviate too much from the normal levels the likelihood of cyst formation increases[7-12]. In addition, the context of the renal tissue is crucial in determining whether or not cyst formation occurs and at what growth rate this process takes place. Under normal conditions the adult kidney is relatively resistant to cyst formation but during renal development, renal injury or during continuous stress on renal tissue imposed by existing cysts, cells are prone to take part in cyst formation once they have lost Polycystin function[13-18].

Multiple signaling pathways, such as mTOR, cAMP, Ca^{2+}, Wnt, STAT3 and Src/Ras/Raf/MEK/ERK, among others, seem to be involved in driving cyst formation[19]. In addition, we showed in a previous study that transforming growth factor-β (TGFβ) signaling may also play a role in PKD[20]. Following binding of the TGFβ ligands (TGFβ1, 2 or 3) to the TGFβ type II receptor II (TGFBR2), TGFβ type I receptor (also termed Activin Receptor-like Kinase 5: ALK5) is recruited and phosphorylated, which then phosphorylates SMAD2 and SMAD3. These phosphorylated SMAD2 and SMAD3 (pSMAD2/3) proteins form a complex with SMAD4 and this complex can enter the nucleus to initiate the transcription of various genes[21]. In pathological conditions TGFβ signaling is known to drive fibrosis in various end-stage renal diseases[22-25]. In cancer, TGFβ can either inhibit tumor formation or promote metastasis depending on the specific conditions in the tumor microenvironment. We previously found increased levels of nuclear pSMAD2 also in cystic epithelial cells, suggesting a possible role for TGFβ in these cells[20]. Although TGFβ inhibited cyst formation in 3D-cyst cultures of ADPKD cells[26], the pleiotropic actions of TGFβ renders it difficult to predict the exact role of TGFβ in the context of the polycystic kidney.

To better understand the role of TGFβ signaling in cyst formation, and to assess whether TGFβ signaling can be used as a therapeutic target to inhibit disease progression, we crossbred kidney-specific tamoxifen-inducible *Pkd1* deletion mice (iKsp-*Pkd1*^{del}) with mice in which exon 3 of the *Alk5* gene is flanked by Lox-P sites[13,27]. This allowed us to simultaneously knock-out *Pkd1* and *Alk5* specifically in the renal epithelium and to study the role of TGFβ signaling in cyst formation. However, we show here that the additional inactivation of

Alk5 did not affect the progression of PKD and only mildly affected SMAD2/3 dependent signaling, suggesting that alternative pathways are accountable for these changes. We previously showed increased expression levels of *Inhibin* β*A*[28]. The different subtypes of *Inhibin* β chains are able to form hetero- or homodimers with other *Inhibin* β chains to form different Activins, or they can dimerize with *Inhibin α* to form Inhibins, which antagonize the activity of Activins[29]. Activins are members of the TGFβ superfamily that bind to Activin type II receptors, which results in recruitment of Activin type I receptor (ACVR1B, or ALK4) and subsequent phosphorylation of SMAD2/3[29]. The soluble Activin receptor IIB fusion protein (sActRIIB-Fc) has been used to enhance muscle growth by antagonizing Myostatin, which is a member of the TGFβ superfamily that signals through the ActRIIB receptor and is a negative regulator for muscle growth[30]. Like Myostatin, also Activin A and Activin B signal through Activin II receptors and can be sequestered by sActRIIB-Fc. We show here that treatment with sActRIIB-Fc markedly slows progression of PKD in three different mouse models for PKD. Taken together, our results suggest that the role of TGFβ in renal epithelial cells is limited in the context of PKD. Furthermore, Activins drive the progression of PKD and are highly promising targets for therapeutic intervention.

CONCISE METHODS

Mice and treatments

iKspCre-*Pkd1*^{lox} mice (*Pkd1*-cKO) have a homozygously bred kidney specific tamoxifen inducible Cre[36]. and two *Lox*P sites that flank exons 2-11 of the *Pkd1* gene[13]. For some experiments, these mice were crossed with mice having exon 3 of the *Alk5* gene flanked by *Lox*P sites[27]. to obtain the indicated genotypes. These mice were all on full C57BL6/J genetic background. Oral tamoxifen administration to facilitate gene disruption was done as described previously[36]. The mice received either 200 mg/kg tamoxifen at P40-P42, 150 mg/kg at P18-P20 or 6 mg/kg tamoxifen at P10-12. Tamoxifen administration at these dosages and ages are well tolerated based on careful assessment of behavior, but the P10-12 mice have reduced bodyweights due to the Tamoxifen treatments. Hypomorphic *Pkd1*^{nl,nl} mice have a PGK promoter-driven neomycin-resistance gene that is flanked by *Lox*P sites in intron 1 of the *Pkd1* gene. This neomycin resistance gene causes alternative splicing of the *Pkd1* gene, resulting in reduced expression of *Pkd1*-WT transcripts, which leads to rapid cyst formation starting around P7[10,32]. Male *Pkd1*^{nl,wt} mice on 129Ola/Hsd genetic background were crossed with female *Pkd1*^{nl,wt} mice on C57BL6/J genetic background to generate *Pkd1*^{nl,nl} F1-hybrids having a fixed genetic background of exactly 50% C57BL6/J and 50% 129Ola/Hsd. These F1-hybrids were used in the experiments. Since PKD in male P18-*Pkd1*-cKO mice progresses faster compared to PKD in female P18-*Pkd1*-cKO mice, we only used male mice for the survival experiment to reduce the number of mice needed for the experiment. For the rapid PKD models, male and female mice have a comparable progression rate and both sexes were used.

The recombinant human sActRIIB-Fc protein is a fusion of a human Fc and the ActRIIB receptor and was produced in house in CHO-S cell suspension cultures using chemically defined serum free medium and the protein was purified by affinity chromatography as described in detail in Hulmi *et.al.* 2013[49]. Mice were treated twice a week with intraperitoneal (IP) injections with sActRIIB-Fc either with 1, 3, or 10 mg/kg in PBS. As a control group, mice received IP injections twice a week with PBS.

Blood sampling and blood urea measurements were performed using Reflotron technology (Kerkhof Medical Service) as described previously[16].

Local animal experimental committee of the Leiden University Medical Center and the Commission Biotechnology in Animals of the Dutch Ministry of Agriculture approved the experiments performed.

Gene expression analysis

Kidneys from sacrificed mice were removed, snap-frozen in liquid nitrogen and stored at -80°C until further processing. Kidneys were homogenized using Magnalyser technology (Roche Applied Science) and total RNA was isolated from kidney samples using Tri-Reagent

(Sigma-Aldrich). Gene expression was either measured by Reverse-Transcription-Multiplex-Dependent-Probe-Amplification (RT-MLPA), or by quantitative-PCR (qPCR) as described previously[16]. RT-MLPA: Briefly, 60-120 ng of RNA was used to synthesize cDNA with strand-specific oligonucleotides in a single reaction with Reverse Transcriptase (Promega). Forward probes (oligonucleotides with a universal sequence at the 5'end) and reverse probes (oligonucleotides with a universal sequence at the 3'end) were hybridized directly adjacent to each other onto the cDNA followed by a ligation step and PCR, using a single primer set (forward primer labeled with a 6-Carboxyfluorescein (FAM) or Hexachloro-fluorescein (*HEX*) fluorescent label) designed to simultaneously amplify all ligated probes (MLPA reagents were from MRC-Holland). The PCR fragments were run on a 3730 DNA analyzer (Applied Biosystems) and peak-heights were analyzed using Peak Scanner 2.0 software (Applied Biosystems). *Ywhaz* and *Hprt* served as reference genes and relative peak-ratios were calculated to determine relative gene expression. Probe sequences of the specific genes are available on request. qPCR: cDNA synthesis was done with Transcriptor First Strand cDNA Synthesis Kit (Roche Applied Science) according to the manufacturer's protocol. Quantitative PCR was done on the LightCycler 480 II (Roche Applied Science) using 2x FastStart SYBR-Green Master (Roche Applied Science) according to the manufacturer's protocol. Primer sequences are available upon request. Data was analysed with Lightcycler 480 Software, Version 1.5 (Roche Applied Science). Gene expression was calculated using LinRegPCR method as described previously[50]. and normalized to *Hprt* expression, giving the relative gene expression. Mean gene expression and standard deviation of the treatment groups were calculated.

Histochemistry and cystic, fibrotic, proliferation and apoptotic indices

Kidneys were fixed in buffered 4% formaldehyde solution and embedded in paraffin. Kidney sections (4μm) were stained with standard hematoxylin and eosin (H&E). Total scans from H&E stained kidney sections were used to determine the cystic indices. The cystic index was determined using Image J software (public domain software; National Institutes of Health) and defined as the percentage of cystic area relative to total tissue. The fibrotic index was measured by staining sections with SiriusRed: After deparaffinization, sections were stained with 0.2% Phosphomolybdic acid (1 min.), 0.1% SiriusRed in Picric Acid (90 min.), and then with saturated Picric Acid, followed by standard ethanol/xylol washes and mounting. All sections were stained simultaneously to avoid inter-experimental variation, and all scanned images were processed exactly the same using Photoshop software. Specifically designed color palettes were used to first remove signal within cysts (leaving only the pixels from all tissue), and then that of the tissue except for the red SiriusRed signal (leaving only the SiriusRed signal). Large arteries were removed from the analysis. The ratio (SiriusRed_pixels vs Complete_tissue_pixels) of the number of pixels were calculated as a percentage and was defined as the fibrotic index. The proliferation index was determined on the basis of

immunohistochemical staining with Ki67 (NCL Ki67p; Nova Castra) as described previously[31]. The apoptotic index was determined in a similar fashion like the proliferation index, only then using Rabbit anti cleaved caspase 3 (9661; Cell Signaling). To determine from which segment of the nephron cysts originate in the kidneys of the P18-*Pkd1*-cKO mice, we performed marker staining with rabbit anti-megalin (1:500; Pathology LUMC, Leiden) to detect proximal tubular cysts, goat anti-Tamm Horsfall protein (uromodulin, 1:500; Organon Teknika-Cappel), to detect distal tubular cysts, or rabbit antiaquaporin-2 (1:4,000; Calbiochem) to detect collecting duct cysts, as described previously[31].

Cell culture and Western blotting

For *in-vitro* analysis, primary cells were generated from the cortexes of kidneys of tamoxifen treated iKspCre;*Pkd1*^{lox,lox} and iKspCre;*Pkd1*^{lox,lox};*Alk5*^{lox,lox} mice. In addition, mouse *Pkd1*$^{-/-}$ and *Pkd1*$^{+/+}$ proximal tubular epithelial cells were cultured and processed as described previously[31]. Western blotting was performed on crude protein extracts using standard procedures and as described previously using an anti-phospho-SMAD2 antibody[51], an anti-αTubulin antibody (CP06, Calbiochem), and a total-SMAD2 antibody (3103 Cell Signaling Technologies)[20]. For optimal performance using westernblot analysis of tissue extracts, TGX gradient gels were used from BioRad. Densitometric analysis was carried out using Odyssey technology (Licor-biosciences).

Statistical Analysis

Differences between survival curves were tested with the generalized Wilcoxon test. All other group comparisons were tested using two-tailed t tests.

RESULTS

TGFBRI (ALK5) ablation in conditional Pkd1 deletion mice.

To better understand the role of TGFβ signaling specifically in the renal epithelium during cystogenesis, we crossbred kidney-specific-tamoxifen-inducible-Cre-*Pkd1*^{lox} mice (iKspCre-*Pkd1*^{lox,lox}) with mice in which exon 3 of the *Alk5* gene is flanked by *Lox*P sites[13,27]. As such, we generated iKspCre-*Pkd1*^{lox,lox} and iKspCre-*Pkd1*^{lox,lox};*Alk5*^{lox,wt} and iKspCre-*Pkd1*^{lox,lox};*Alk5*^{lox,lox} mice. Eleven weeks following tamoxifen administration at Post-Natal day (P) 40, 41 and 42 (i.e. these mice have mild tubular dilations), *Alk5* expression was reduced in iKspCre-*Pkd1*^{lox,lox};*Alk5*^{lox,wt} mice and was reduced more in iKspCre-*Pkd1*^{lox,lox};*Alk5*^{lox,lox} mice, indicating homozygous inactivation of *Alk5* (Figure 1A). Next, we followed mice until the onset of end-stage PKD (defined as Blood Urea (BU) concentration > 20 mmol/l). Both iKspCre-*Pkd1*^{lox,lox} (from now on referred to as *Pkd1*-cKO) and iKspCre-*Pkd1*^{lox,lox};*Alk5*^{lox,lox} mice (from now on referred to as *Pkd1*;*Alk5*-cKO) had a similar progression rate of PKD and although there was a trend that the *Pkd1;Alk5*-cKO mice had slightly higher 2KW/BW%, this was not significant. Also renal histology was not different, indicating that renal epithelial *Alk5* expression does not play a significant role in the progression of PKD (Figure 1B-D).

We next measured the expression of SMAD2/3-dependent target genes by Reverse-transcriptase-ligation-dependent-probe-amplification (RT-MLPA), which were massively upregulated in cystic kidneys of *Pkd1*-cKO mice compared to control mice (Figure 1E). Surprisingly, however, *Pkd1*;*Alk5*-cKO mice showed a similar upregulation, being only slightly less compared to *Pkd1*-cKO mice (Figure 1E). These results indicate that the role of renal epithelial *Alk5* expression on cystogenesis or SMAD2/3-dependent signaling is limited, and suggests the involvement of other pathways to account for these changes during cyst formation.

Activin expression is increased in PKD and kidney cells respond to Activin.

We previously found increased *Inhibin* β*A* expression in PKD samples, which is a member of the TGFβ super family[28]. Upon dimerization, Inhibin β chains can form different Activin subtypes, which can drive SMAD2/3 phosphorylation through the *ALK4* and *ACTRII* receptors[29]. Here, we analyzed both *Inhibin* β*A* and *Inhibin* β*B* expression and found that the expression of both ligands were elevated at end-stage PKD (defined as BU > 20 mmol/L, which occurs approximately 16 weeks after Tamoxifen)[31]. but also at early-stage PKD (11 weeks after Tamoxifen administration, at which the mice have mild tubular dilations)[31], suggesting a possible role for Activin signaling already at the early stages of cyst formation (Figure 2A and 2B).

Cultured primary cells isolated from total kidneys from tamoxifen treated *Pkd1*-cKO or *Pkd1*;*Alk5*-cKO mice, and cultured *Pkd1*$^{+/+}$ or *Pkd1*$^{-/-}$ immortalized proximal tubular epithelial cells were all capable to respond to ActivinA and TGFβ by inducing SMAD2 phosphorylation

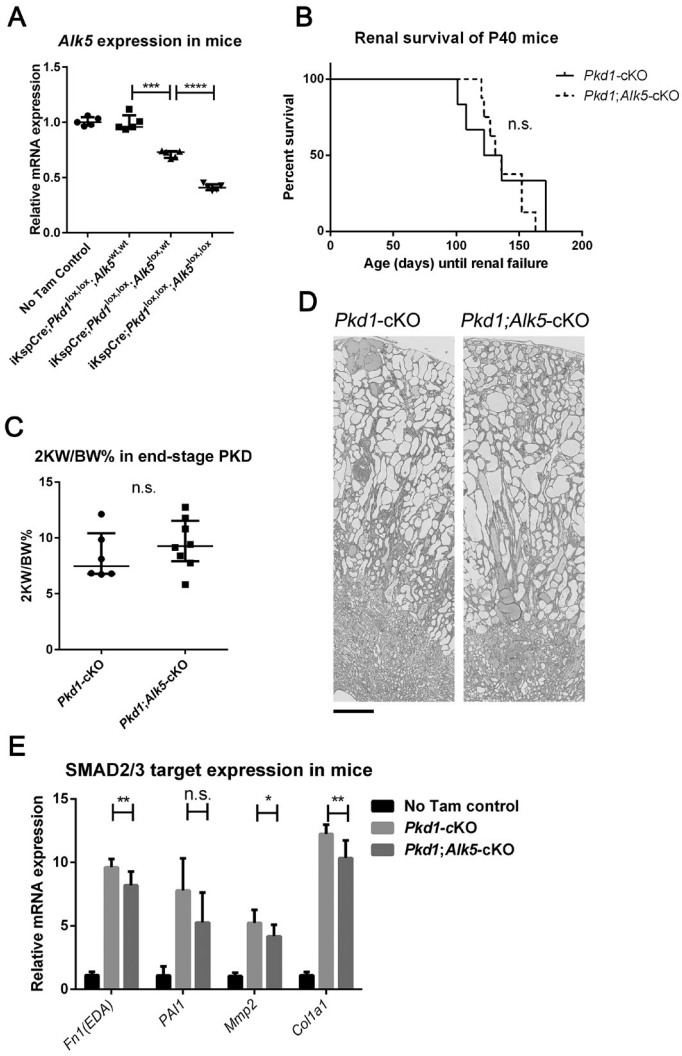

Figure 1. Conditional ablation of *Alk5* in the renal epithelium does not affect PKD.

(A) Renal expression of *Alk5* in mice of different genotypes (iKspCre;*Pkd1*^{lox,lox};*Alk5*^{wt,wt}, iKspCre;*Pkd1*^{lox,lox};*Alk5*^{lox,wt} and iKspCre;*Pkd1*^{lox,lox};*Alk5*^{lox,lox}) treated with Tamoxifen at P40, 41, 42 and euthanized 11 weeks after Tamoxifen. Adult iKspCre;*Pkd1*^{lox,lox};*Alk5*^{wt,wt} mice without Tamoxifen treatments served as a control (No Tam Control). Expression was measured by Reverse Transcriptase Multiplex Ligation-dependent Probe Amplification (RT-MLPA). *Hprt* and *ywhaz* served as housekeeping genes to correct for cDNA input (n = 5 mice per group). Error bars indicate interquartile range (B) Renal survival analysis (a Blood Urea level (BU) of 20 mmol/L served as a cutoff point) of *Pkd1*-cKO (n = 6 mice) and *Pkd1;Alk5*-cKO (n = 8 mice) mice that were treated with Tamoxifen at P40, 41, 42. (C) The ratio of the kidney weight to body weight expressed as a percentage (2 KW/BW%) of the mice also depicted in Figure 1B. Error bars indicate interquartile range (D) Representative hematoxylin and eosin-stained kidney sections from end-stage polycystic kidneys of *Pkd1*-cKO and *Pkd1;Alk5*-cKO mice. Scale bar: 500 μm. (E) Expression of the SMAD2/3 target genes the EDA splice form of *fibronectin 1 (Fn1(EDA)), plasminogen activator inhibitor-1 (PAI1),* matrix metalloproteinase-2 *(Mmp2)* and *collagen, type I, α1 (Col1α1)* from kidneys of P40 Tamoxifen treated *Pkd1*-cKO mice (n = 5) and *Pkd1;Alk5*-cKO mice (n = 5) that were euthanized at the onset of renal failure caused by severe PKD (defined as having BU levels above 20 mmol/L). Expression of the genes of *Pkd1*-cKO mice (n = 5) without Tamoxifen (No Tam Control) are also shown. Expression was measured by Reverse Transcriptase Multiplex Ligation-dependent Probe Amplification (RT-MLPA). *Hprt* and *ywhaz* served as housekeeping genes to correct for cDNA input. Error bars indicate standard deviations. (n.s. indicates Not Significant, * indicates $P < 0.05$, *** indicates $P < 0.001$, **** indicates $P < 0.0001$).

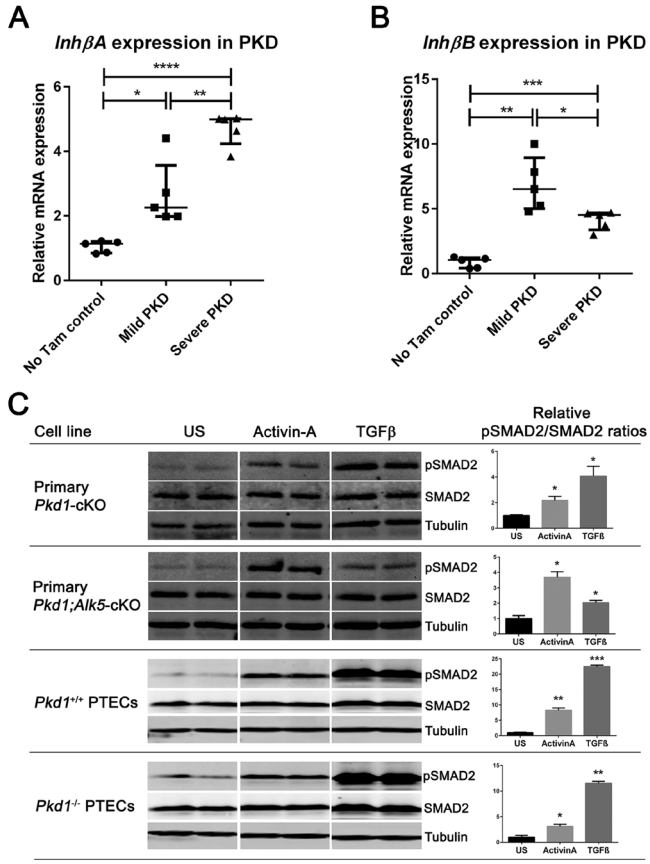

Figure 2. Activin expression in PKD kidneys and stimulation of cells. (A-B) *Inh*βA (A) and *Inh*βB (B) mRNA expression in kidneys from P40 Tamoxifen treated *Pkd1*-cKO mice euthanized 11 weeks after Tamoxifen (Mild PKD) or at the onset of renal failure (defined as having BU levels above 20 mmol/L) (Severe PKD) (*n* = 5 mice per group). Expression of the genes of *Pkd1*-cKO mice without Tamoxifen (No Tam Control) served as a reference. The expression was measured by qPCR. *Hprt* served as a housekeeping gene to correct for cDNA input. Error bars indicate interquartile range. * indicates $P < 0.05$, ** indicates $P < 0.01$, *** indicates $P < 0.001$, **** indicates $P < 0.0001$. (C) Western blot and quantification of pSMAD2 and total SMAD2 on crude extracts from primary cells from a kidney of one P40 Tamoxifen treated *Pkd1*-cKO (Primary *Pkd1*-cKO), and of one P40 Tamoxifen treated *Pkd1;Alk5*-cKO mouse (Primary *Pkd1;Alk5*-cKO). Also results of crude extracts of $Pkd1^{+/+}$ ($Pkd1^{+/+}$ PTECs) or $Pkd1^{-/-}$ ($Pkd1^{-/-}$ PTECs) mouse Proximal Tubular Epithelial Kidney cells (PTECs) are shown. All cell lines were either left unstimulated (US), or were stimulated with 5 ng/ml TGFβ1, or with 100 ng/ml Activin-A. Each stimulation experiment on the above mentioned cell lines was performed at least three times. A representative experiment with two replicates of the same cell line of each condition are shown in which tubulin served as a loading control. pSMAD2/SMAD2 ratios are shown and were normalized to the unstimulated cells that were set to 1. * indicates $P < 0.05$, ** indicates $P < 0.01$, *** indicates $P < 0.001$ compared with the unstimulated control.

(Figure 2C). The response pattern of the primary kidney cells from tamoxifen treated *Pkd1;Alk5*-cKO mice indicated reduced sensitivity to TGFβ, which is likely caused by the conditional ablation of *Alk5* in the majority of cells (Figure 1A and 2C). Although these *in vitro* experiments do not recapitulate the complex signaling in the context of a cystic kidney, these results indicate that renal epithelial cells can potentially be stimulated by Activins and TGFβ. To further assess the role of Activins in cystic kidneys we aimed to inhibit Activins in mouse models for PKD, using a soluble Activin ligand trap.

sActRIIB-Fc inhibits disease progression in two mouse models with rapid PKD progression. To explore the role of Activin signaling in PKD and to determine whether Activins can be used as a therapeutic target for PKD, we used a soluble Activin ligand trap (sActRIIB-Fc). We first used the *Pkd1*-cKO model in which we inactivated *Pkd1* by tamoxifen administration at P10-12. *Pkd1*-inactivation before P14 results in rapid cyst formation as opposed to *Pkd1* inactivation after P14[13,14]. As expected, at age P33, mice that received phosphate buffered saline (PBS) had increased 2-kidney to bodyweight ratios (2KW/BW%), cystic indices (CI) and increased Blood-Urea (BU) levels indicating deteriorating renal function (Figure 3A-C). By contrast, mice that also received biweekly intraperitoneal (IP) injections of 3 or 10 mg/kg sActRIIB-Fc, starting at P14 until the end of the experiment at age P33, showed improvement in all of these parameters and improvement of renal histology (Figure 3A-D and Supplemental Figure 1).

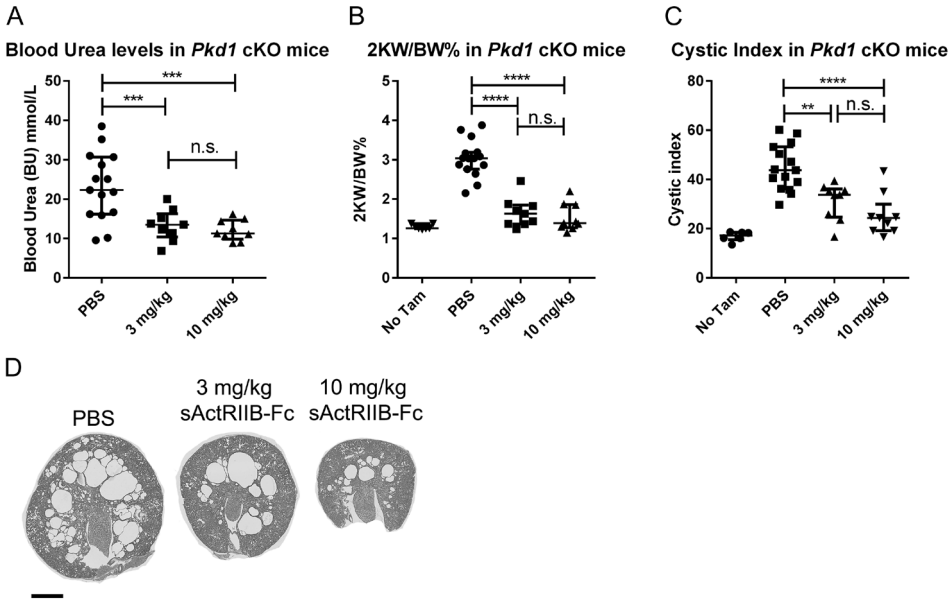

Figure 3. Antagonizing Activin signaling effectively inhibits cyst progression in conditional *Pkd1*-deletion mice. (A-C) *Pkd1*-cKO mice (*n* = 15 mice; 8 males and 7 females) were treated with tamoxifen at P10,11,12 and euthanized at P33. Mice that were additionally treated with 3 (*n* = 9 mice; 4 males and 5 females) or 10 mg/kg (*n* = 9 mice; 4 males and 5 females) sActRIIB-Fc from P14-P33 had improved renal function (A), significantly lower kidney weights (B), and cystic indices (C). (D) Shown are representative images of the renal histology of the different treatment groups. The mice treated with 3 or 10 mg/kg sActRIIB-Fc had improved renal histology compared with PBS treated mice. Histology of all mice is shown in Supplemental Figure 1. Scale bar: 1 mm. (n.s. indicates Not Significant, ** indicates $P < 0.01$, *** indicates $P < 0.001$, **** indicates $P < 0.0001$, error bars indicate interquartile range).

To test if the cyst reducing properties of sActRIIB-Fc are not specific for just the conditional *Pkd1*-deletion model, we also used a different model for PKD. To this end, we tested the efficacy of sActRIIB-Fc also on hypomorphic *Pkd1*^{nl,nl} mice. These mice have in all of their cells only about 15-20% of normal *Pkd1* expression and have already small cysts at age P7 and by the age of P20 they have developed massive PKD[10,32]. In addition, we bred these mice on a different genetic background (i.e. the *Pkd1*^{nl,nl} mice in this study were F1-hybrids having a fixed genetic background of exactly 50% C57BL6/J and 50% 129Ola/Hsd genetic background). We treated these mice with in total 4 IP injections of 0, 1 or 10 mg/kg sActRIIB-Fc between P10 and P21. Even this short treatment regimen showed significant improvements in renal function and size (Figure 4A-D and Supplemental Figure 2).

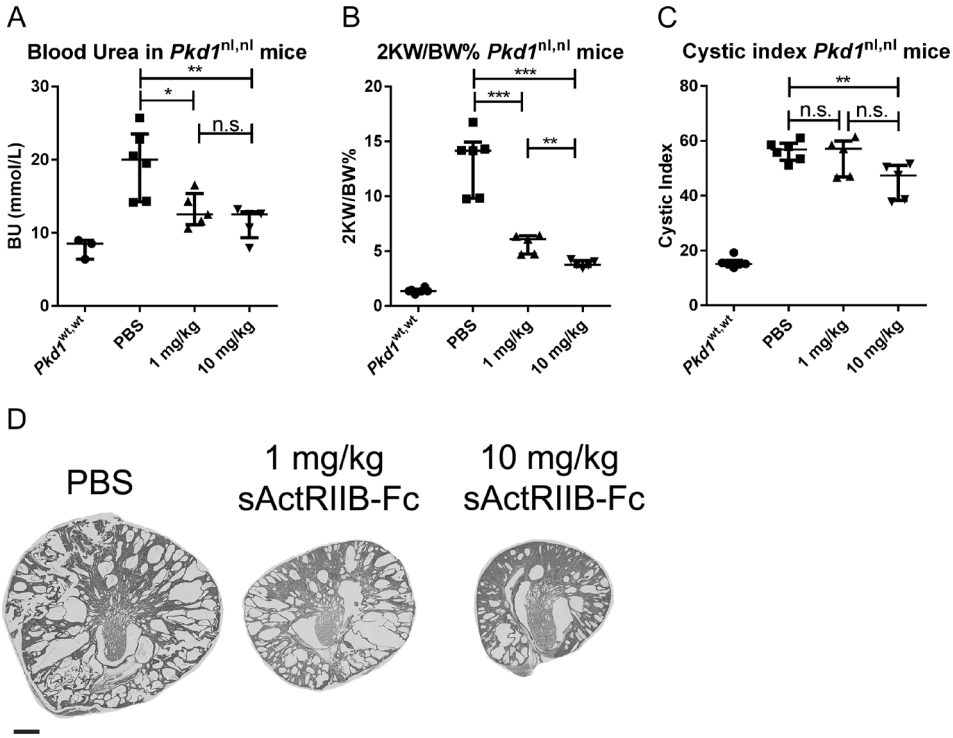

Figure 4. Antagonizing Activin signaling effectively inhibits cyst progression in hypomorphic *Pkd1* mice.

(A-C) Hypomorphic *Pkd1*^{nl,nl} mice bred on a mixed genetic background of C57BL6/J and 129Ola/Hsd were treated with in total 4 IP injections of 0 (*n* = 6 mice; 1 male and 5 females), 1 (*n* = 5 mice; 2 males and 3 females) or 10 (*n* = 5 mice; 2 males and 3 females) mg/kg sActRIIB-Fc between P10 and P21. Shown are BU levels (A), 2KW/BW% (B) and cystic indices (C). (D) Representative H&E stained kidney sections of the hypomorphic mice treated with the indicated dosages of sActRIIB-Fc. Histology of all mice is shown in Supplemental Figure 2. Scale bar: 1 mm. (n.s. indicates Not Significant, * indicates $P < 0.05$, ** indicates $P < 0.01$, *** indicates $P < 0.001$, error bars indicate interquartile range).

The improved renal health by sActRIIB-Fc treatment is associated with reduced fibrosis and SMAD2/3 dependent signaling.

The PKD phenotype is generally associated with increased proliferation and expression of SMAD2/3 target genes, which could be a reflection of increased fibrosis[20].. We therefore measured the proliferation, apoptotic and fibrotic index of the P10-*Pkd1*-cKO mice. The proliferation indices were determined by taking the ratio of Ki67 positive and Ki67 negative nuclei of sections that were stained for this proliferation marker. The apoptotic index was measured in a similar fashion using sections stained for cleaved Caspase-3, which is a marker for apoptosis. The fibrotic index was measured by determining the amount of Collagen deposition in kidney sections using Sirius Red stainings. The number of apoptotic cells increased in mice with *Pkd1*-cKO compared to control mice without *Pkd1*-cKO, but the sActRIIB-Fc treatments did not significantly affect apoptosis and there were no statistically significant differences in proliferation between the tested groups (Figure 5A-B). However, the fibrotic index was clearly reduced in the 3 and 10 mg/kg sActRIIB-Fc treated mice, which correlated with reduced expression of *collagen, type I, α1 (Col1α1),* and *plasminogen activator inhibitor-1 (PAI1)*. However, compared to the PBS treated mice, the expression of the EDA splice form of *fibronectin 1 (Fn1(EDA))* was only significantly reduced in mice treated with 10 mg/kg sActRIIB-Fc (Figure 5C-D and Supplemental Figure 3). Since, pSMAD2 protein levels in kidney extracts of the P10-*Pkd1*-cKO mice, as assessed by western blotting, were below the detection limit, we were not able to connect the expression of these genes to the levels of pSMAD2/3 (data not shown). We therefore also immunoblotted kidney extracts of the *Pkd1*^{nl,nl} mice that were treated with PBS, 1 or 10 mg/kg sActRIIB-Fc. pSMAD2 was only detected in PBS treated *Pkd1*^{nl,nl} mice, and dropped below the detection limit in the sActRIIB-Fc treated mice (Figure 5E-F). Interestingly, also total SMAD2 levels were increased in *Pkd1*^{nl,nl} mice compared to WT-control mice, which were reduced in the sActRIIB-Fc treated mice (Figure 5E and 5G). Taken together, these results indicate that the reduced cystic load achieved by sActRIIB-Fc treatment, is associated with reduced SMAD2/3 dependent signaling and fibrosis.

sActRIIB-Fc treatment slows PKD in adult onset Pkd1-cKO mice.

To investigate if Activin inhibition could also slow disease progression in an adult onset model for PKD, we conducted a survival experiment. We first treated male *Pkd1*-cKO mice with Tamoxifen at P18, 19 and 20 to inactivate *Pkd1*. These mice have a young adult onset of PKD with cyst formation from all tubular segments (Supplemental Figure 4, and Leonhard W.N., Peters D.J.M.; manuscript in preparation). After randomization of the mice in the different groups, biweekly treatments with PBS (PBS control) or 3 mg/kg sActRIIB-Fc were started at P46 (long treatment). In addition, one group of mice that received PBS from P46, switched to 3 mg/kg sActRIIB-Fc treatment at P74 (late treatment). From approximately P78 the renal function of the mice was monitored weekly by measuring Blood Urea (BU) levels. BU of 20

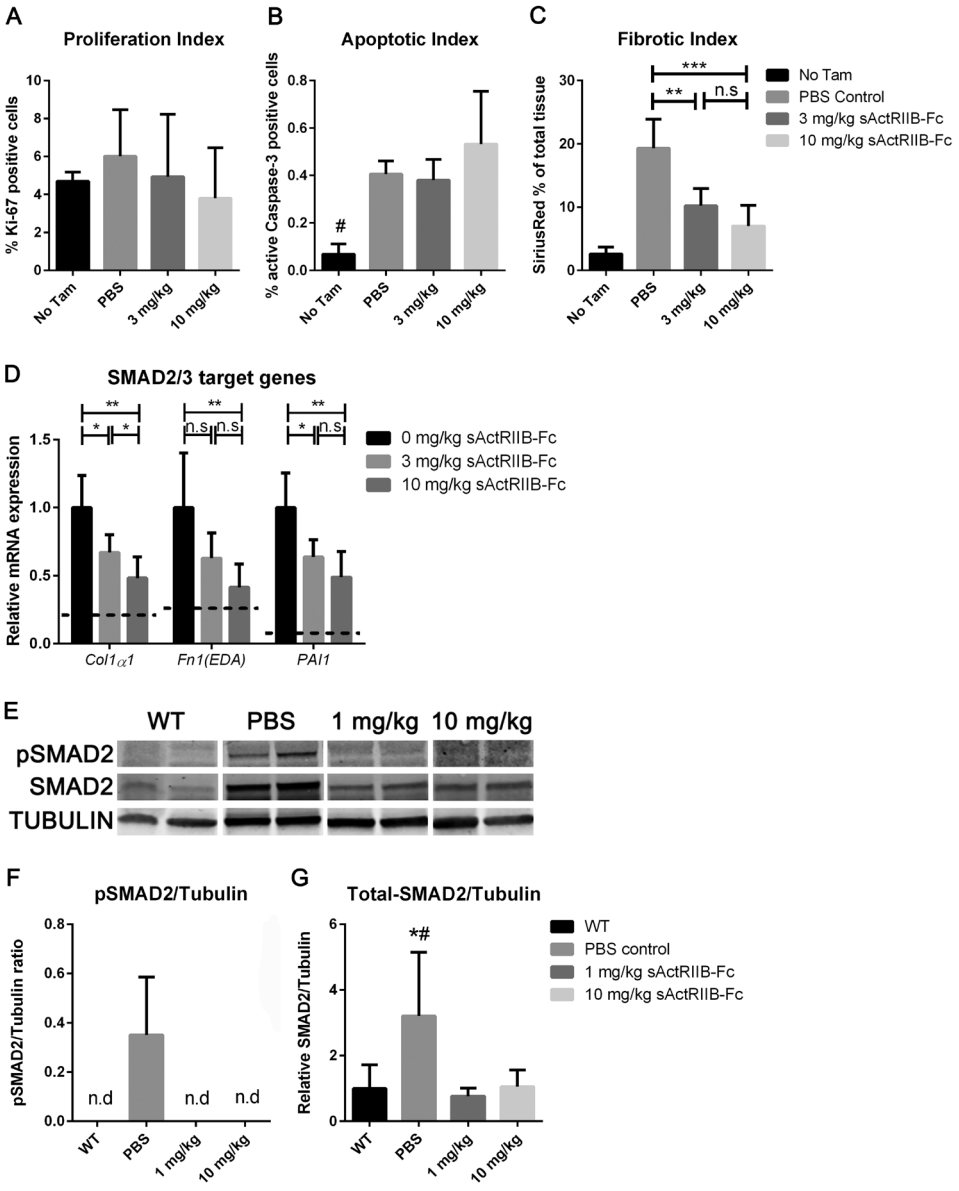

Figure 5. The improved renal phenotype by sActRIIB-Fc is associated with reduced SMAD2/3 signaling.

(A-B) The proliferation index and apoptotic index was measured in renal samples of the P10-*Pkd1*-cKO mice in the indicated groups. (C) Collagen deposition was measured by SiriusRed staining (example images are shown in Supplemental Figure 3) from renal sections of the P10-*Pkd1*-cKO mice in the indicated groups. (D) The expression of the EDA splice form of *fibronectin 1 (Fn1(EDA)), plasminogen activator inhibitor-1 (PAI1),* and *collagen, type I, α1 (Col1α1)* from kidneys of the P10-*Pkd1*-cKO mice that were treated with 0, 3 or 10 mg/kg sActRIIB-Fc was measured by qPCR. The dotted lines indicate the expression levels of genotype and age matched *Pkd1*-floxed mice without ➤

mmol/L was used as a cutoff point to pinpoint the onset of renal failure. The median survival in days after the start of the long-treatment-regimen was 55 days in the PBS group and was significantly postponed to 97 days in the sActRIIB-Fc treated group (Figure 6). sActRIIB-Fc treatments starting at 74 days did not significantly slow PKD, suggesting that the effect of sActRIIB-Fc is more prominent during the milder stages of PKD (Figure 6). Collectively, the improvement in renal health in three distinct models for PKD by sActRIIB-Fc treatment, suggests that Activin inhibition is an attractive approach to inhibit ADPKD.

Additional effects of sActRIIB-Fc.

Several studies showed that sActRIIB-Fc treatment increases bodyweight, which is primarily caused by increased muscle size due to the ability of sActRIIB-Fc to antagonize Myostatin, which is a negative regulator for muscle growth. Since the 2KW/BW% is influenced by the bodyweight, we summarized the bodyweights, kidney weights, 2KW/BW% and cystic indices of all mice in Supplemental Figure 5. Whereas the bodyweights at the start of each experiment generally were comparable between the groups, at the end of the experiments the bodyweights of the sActRIIB-Fc treated mice tended to be slightly higher. This was more prominent in the long-term sActRIIB-Fc treated P18-*Pkd1*-cKO mice. Besides the effect on bodyweight, the data summary confirms that sActRIIB-Fc treatment reduced kidney weights and cystic indices, or delayed the onset of renal failure.

We measured the weight of the quadriceps's in the P10-*Pkd1*-cKO mice that were treated with 10 mg/kg sActRIIB-Fc and confirmed that muscle size was increased, which could explain the relative higher bodyweights of the sActRIIB-Fc treated mice in this study (Supplemental Figure 6A). Overall behavior and morphology was normal in sActRIIB-Fc treated mice, and there were no obvious changes in liver, spleen or pancreas tissues of the mice (data not shown). In addition, there was no sign of liver toxicity as the alanine aminotransferase (ALT) levels of the sActRIIB-Fc treated mice in the survival experiment were similar or slightly lower compared to PBS treated mice (Supplemental Figure 6).

◀ tamoxifen. *Hprt* served as a housekeeping gene to correct for cDNA input. (E-G) Renal extracts from $Pkd1^{nl,nl}$ mice were immunoblotted and stained for phosphorylated SMAD2 (pSMAD2), total SMAD2 (SMAD2) or TUBULIN as a loading control. (E) a representative immunoblot of the indicated samples and protein expressions. (F-G) Quantification of pSMAD2/TUBULIN ratios (F) or SMAD2/TUBULIN ratios (G). pSMAD2 was only detected in $Pkd1^{nl,nl}$ mice that were treated with PBS.

For all quantifications in this Figure: $n = 5$ mice for all groups. These mice were representative for the actual averages based on the 2KW/BW%. n.d. = not detected, n.s. = not significant, * indicates $P < 0.05$, ** indicates $P < 0.01$, *** indicates $P < 0.001$, # indicates: the 'No Tam' control group had significantly lower numbers of apoptotic cells compared to each of the other groups $P < 0.05$. *# indicates: PBS treatment compared to either 1 mg/kg or 10 mg/kg sActRIIB-Fc treated $Pkd1^{nl,nl}$ mice, $P < 0.05$. Error bars indicate standard deviations).

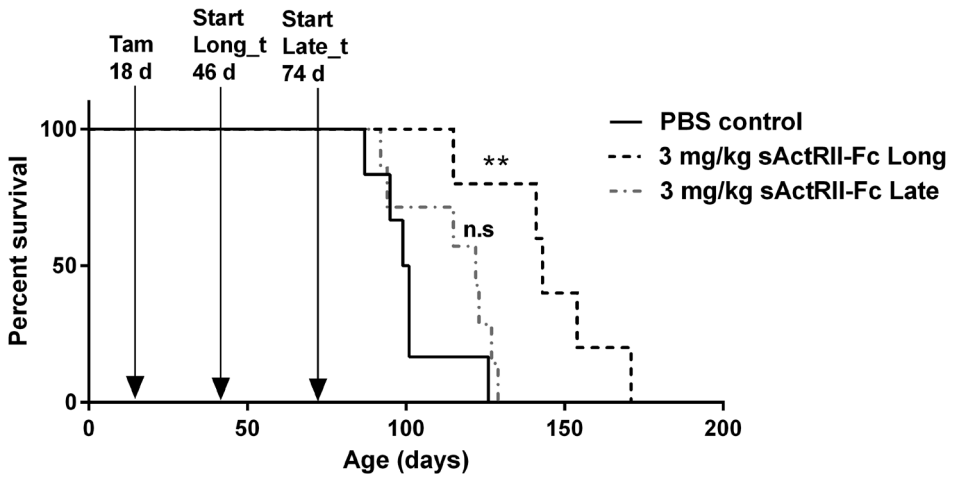

Figure 6. sActRIIB-Fc treatment slows PKD in an adult onset model for PKD.

Survival analyses of *Pkd1*-cKO mice treated with Tamoxifen at P18. PBS (PBS control) or sActRIIB-Fc (3 mg/kg sActRIIB long) treatment was started at 46 days of age. However, 7 mice switched from PBS treatment to sActRIIB-Fc treatment at 74 days of age (3 mg/kg sActRII Late). BU was measured weekly and the onset of renal failure was defined as having a BU > 20 mmol/L. From the start of the first treatment at age 46 days, the median survival of PBS treated mice (n = 6 mice) was 54 days (age 100 days), median survival of late treated mice (n = 7 mice) was 76 days (age 122 days) and median survival of long treated mice (n = 5 mice) was 97 days (age 143 days). ** indicates $P < 0.01$, n.s. indicates not significant.

DISCUSSION

The data presented in this study point to Activins as novel players in driving the progression of PKD. Treatment with sActRIIB-Fc, which is capable of sequestering Activins, inhibited cystogenesis in three distinct mouse models of PKD. At present there is not yet an approved, safe and effective therapy for the treatment of ADPKD, although a few completed and ongoing clinical trials with the primary focus of inhibiting cAMP have shown clinical benefit in ADPKD patients[33-35]. Many other PKD related signaling pathways are continued to be studied as potential targets for the treatment of ADPKD[19].

In this study, we focused on TGFβ and Activins, which are members of the TGFβ superfamily that signal through their receptors and can drive SMAD2/3 phosphorylation. Increased expression of SMAD2/3 target genes and extracellular matrix remodeling enzymes, expansion of the interstitial space followed by fibrosis, and the accumulation of pSMAD2 in cystic epithelial cells, suggest their involvement in ADPKD[20,25]. Since TGFβ is involved in driving fibrosis in different chronic kidney diseases, its role likely has overlap with fibrosis in ADPKD[22-25]. The role of TGFβ in driving cyst formation is less well studied, although in 3D-cyst cultures of ADPKD cells, TGFβ inhibited cyst formation[26]. To study the specific role of TGFβ in renal epithelial cells in the context of a PKD phenotype, we ablated *Tgf*βRI (*Alk5*) together with *Pkd1* using a previously developed renal epithelial specific and tamoxifen inducible Cre system[13,27,36]. As expected, primary cells from *Pkd1*-cKO mice were capable to respond to TGFβ, whereas this response was abrogated in primary cells from *Pkd1:Alk5*-cKO mice. By contrast, in the PKD context *in vivo*, additional ablation of *Alk5* only minimally affected the massive upregulation of SMAD2/3 target genes. We cannot exclude that other cell types may be involved in the increased expression of SMAD2/3 target genes in end-stage PKD. Another explanation could be that *Alk5* independent pathways contribute to these changes. Either way, our results indicate that renal epithelial expression of *Alk5* does not contribute significantly to cyst progression in adult *Pkd1*-cKO mice. These data and the observed increased *Inh*βA and *Inh*βB expression in PKD, pointed us to Activins, which, like the TGFβ ligands, are members of the TGFβ superfamily[29].

Activins are composed of two Inhibin β chains and can stimulate SMAD2/3 phosphorylation via the Activin type II receptors and ALK4[29]. These ligands play key roles in cancer and in wound repair programs[37]. Of interest, mutations in the von Hippel-Lindau tumor suppressor gene stimulates hypoxia-inducible factor (HIF)-dependent expression of Activin B, which promoted tumor growth[38]. However, whether Activins stimulate or inhibit epithelial repair upon damage and how they are involved in fibrosis and cancer seems to differ among different tissues and also depends on the specific context of the tissue, the interplay between stromal and parenchymal cells, and on the expression of other members of the

TGFβ superfamily[37]. It is therefore difficult to predict the exact role of Activins in the context of PKD. Since cyst formation is suggested to be a state of chaotic repair[39], it is tempting to speculate that the increased Activin expression in PKD is in fact an underlying cause of this process. To test if blocking Activin signaling could be a therapeutic strategy to treat ADPKD, we treated three different PKD mouse models with sActRIIB-Fc, which can be used as a soluble Activin ligand-trap. In all of these models, sActRIIB-Fc treatment was associated with slower cyst progression compared to PBS treated littermates. Although in most analyses there was a trend towards a dose dependent response of the sActRIIB-Fc treatments, this did not reach statistical significance. The proliferation and apoptotic index varied between the animals and were not clearly different between PBS or sActRIIB-Fc treated P10-*Pkd1*-cKO littermates. Although these data suggest that sActRIIB-Fc treatment did not significantly affect these processes, we cannot exclude that sActRIIB-Fc affects proliferation and/or apoptosis during any other time-point throughout the course of the development of PKD. Whether this is the case, remains to be investigated. However, the slower onset of PKD by sActRIIB-Fc treatment, was associated with reduced SMAD2 expression, reduced SMAD2 phosphorylation, reduced SMAD2/3 target gene expression and reduced Collagen deposition, which is in line with the concept of the ability of sActRIIB-Fc to sequester Activin ligands, which are increased in PKD. However, sActRIIB-Fc is also known to sequester other ligands of the TGFβ superfamily such as Myostatin, GDF11 and, with lower efficiencies, also a number of BMP's[40,41]. In-house RNAseq data of mice with PKD, showed that Myostatin is not expressed in kidneys with or without PKD, and that GDF11 expression is low and unchanged throughout the course of PKD progression (Malas *et.al.* unpublished). BMP's primarily signal through SMAD1/5/8, which has been observed not to be significantly changed in two mouse models of PKD, suggesting that the cyst reducing properties of sActRIIB-Fc are not likely mediated by its limited ability to sequester BMP's[20]. sActRIIB-Fc treatment indeed increased muscle mass and bodyweight, which is likely due to the ability of sActRIIB-Fc to sequester the negative regulator of muscle growth Myostatin. In addition, the ligand traps, including ActRIIA and ActRIIB variants, have been observed before to also prolong survival in cancer cachexia models, improve bone mineralization in models with established bone loss, suppress LPS-induced lung inflammation, improve obesity and obesity-linked metabolic disease, and to correct ineffective erythropoiesis in mice with beta-thalassemia by growth and differentiation factor (GDF11) inactivation[42-46]. We therefore cannot fully exclude that the renal cyst reducing property of sActRIIB-Fc is actually secondary to effects of sActRIIB-Fc on other organs such as the observed skeletal muscle hypertrophy. However, given the increase in the expression of Activins within the cystic kidney, the reduction of SMAD2/3 dependent signaling and collagen deposition upon sActRIIB-Fc treatment, our data point to a scenario in which the renal cyst reducing property of sActRIIB-Fc is caused by its ability to trap Activin ligands within the (pre)-cystic kidney. How Activins and their downstream signaling cascades are interconnected with other cyst inducing pathways, and how the

combined processes induce the development of cysts is not yet clearly understood and remains to be elucidated.

Currently, several soluble-receptor-ligand-traps are being tested in clinical trials for various purposes[47,48]. One phase II trial to improve muscle function in Duchenne Muscular Dystrophy patients using a sActRIIB-Fc variant had to be terminated because of side effects, which included bleedings of the nose and gum (NCT01099761). However, another 4-month phase I trial assessing the safety of a sActRIIA variant in healthy postmenopausal women up to a dosage of 1 mg/kg, reported that the treatments were safe and well tolerated[48]. A number of phase II trials are currently being undertaken to further assess the therapeutic potential of the sActRIIA variant, primarily in diseases involving anemia. These studies will shed more light on the tolerability of treatments with such ligand traps.

Since ADPKD patients likely require years of treatment, the treatment should have an excellent safety profile. The continuous improvements in the strategies to slow ADPKD are highly encouraging and will likely lead to a safe and effective therapy. Although it remains to be clarified if targeting Activins can be applied safely in humans for longer periods, the effective inhibition of PKD in three mouse models by sActRIIB-Fc points to Activins as potentially important targets for ADPKD treatment.

Acknowledgements
This research was funded by the Dutch Kidney Foundation grant NSN 14OI12 and IP11.34 (WNL, JP) and partially supported by the Netherlands Organisation for Scientific Research (Earth and Life Sciences-820.02.016) (SJK), NSN consortium project CP10.12 (Developing Interventions to hold progression of Polycystic Kidney Disease) (KV) and the Dutch Technology Foundation (Stichting Technische Wetenschappen) Project 11823 (WNL, FB) which is part of The Netherlands Organization for Scientific Research. We are grateful to Dr. Stefan Karsson for providing us with *Alk5* floxed mice.

Disclosures
None.

REFERENCES

1. Peters D.J.M. & Sandkuijl L.A. Genetic heterogeneity of polycystic kidney disease in Europe. *Contributions to Nephrology.* **97**, 128-139 (1992). *Polycystic Kidney Disease. 2nd International Workshop of the European Concerted Action Towards Prevention of Renal Failure Caused by Polycystic Kidney Disease, Parma, September 1991.* (eds: Breuning M.H., Devoto M., Romeo G.; Karger, Basel, 1992).
2. The European Polycystic Kidney Disease Consortium *et al.* The polycystic kidney disease 1 gene encodes a 14 kb transcript and lies within a duplicated region on chromosome 16. *Cell* **77**, 881-894 (1994).
3. Mochizuki T. *et al.* PKD2, a gene for polycystic kidney disease that encodes an integral membrane protein. *Science* **272**, 1339-1342 (1996).
4. Gabow P.A. Autosomal dominant polycystic kidney disease: More than a renal disease. *Am J Kidney Dis* **16**, 403-413 (1990).
5. Grantham J.J., Geiser J.L., & Evan A.P. Cyst formation and growth in autosomal dominant polycystic kidney disease. *Kidney Int.* **31**, 1145-1152 (1987).
6. Grantham J.J. *et al.* Detected renal cysts are tips of the iceberg in adults with ADPKD. *Clin. J. Am. Soc. Nephrol.* **7**, 1087-1093 (2012).
7. Qian F.J., Watnick T.J., Onuchic L.F., & Germino G.G. The molecular basis of focal cyst formation in human autosomal dominant polycystic kidney disease. *Cell* **87**, 979-987 (1996).
8. Wu G. *et al.* Somatic inactivation of Pkd2 results in polycystic kidney disease. *Cell* **93**, 177-188 (1998).
9. Pritchard L. *et al.* A human PKD1 transgene generates functional polycystin-1 in mice and is associated with a cystic phenotype. *Hum. Mol. Genet.* **9**, 2617-2627 (2000).
10. Lantinga-van Leeuwen I.S. *et al.* Lowering of Pkd1 expression is sufficient to cause polycystic kidney disease. *Hum. Mol. Genet.* **13**, 3069-3077 (2004).
11. Jiang S.T. *et al.* Defining a link with autosomal-dominant polycystic kidney disease in mice with congenitally low expression of Pkd1. *Am. J. Pathol.* **168**, 205-220 (2006).
12. Thivierge C. *et al.* Overexpression of PKD1 causes polycystic kidney disease. *Mol. Cell Biol.* **26**, 1538-1548 (2006).
13. Lantinga-van Leeuwen I.S. *et al.* Kidney-specific inactivation of the Pkd1 gene induces rapid cyst formation in developing kidneys and a slow onset of disease in adult mice. *Hum. Mol. Genet.* **16**, 3188-3196 (2007).
14. Piontek K., Menezes L.F., Garcia-Gonzalez M.A., Huso D.L., & Germino G.G. A critical developmental switch defines the kinetics of kidney cyst formation after loss of Pkd1. *Nat. Med.* **13**, 1490-1495 (2007).
15. Patel V. *et al.* Acute kidney injury and aberrant planar cell polarity induce cyst formation in mice lacking renal cilia. *Hum. Mol. Genet.* **17**, 1578-1590 (2008).
16. Happe H. *et al.* Toxic tubular injury in kidneys from Pkd1-deletion mice accelerates cystogenesis accompanied by dysregulated planar cell polarity and canonical Wnt signaling pathways. *Hum. Mol. Genet.* **18**, 2532-2542 (2009).
17. Takakura A. *et al.* Renal injury is a third hit promoting rapid development of adult polycystic kidney disease. *Hum. Mol. Genet.* **18**, 2523-2531 (2009).
18. Leonhard W.N. *et al.* Scattered Deletion of PKD1 in Kidneys Causes a Cystic Snowball Effect and Recapitulates Polycystic Kidney Disease. *J. Am. Soc. Nephrol.* **26**, 1322-1333 (2015).
19. Harris P.C. & Torres V.E. Genetic mechanisms and signaling pathways in autosomal dominant polycystic kidney disease. *J. Clin. Invest* **124**, 2315-2324 (2014).
20. Hassane S. *et al.* Elevated TGFbeta-Smad signalling in experimental Pkd1 models and human patients with polycystic kidney disease. *J. Pathol.* **222**, 21-31 (2010).
21. Ten Dijke P. & Arthur H.M. Extracellular control of TGFbeta signalling in vascular development and disease. *Nat. Rev. Mol. Cell Biol.* **8**, 857-869 (2007).
22. Yamamoto T., Noble N.A., Miller D.E., & Border W.A. Sustained expression of TGF-beta 1 underlies development of progressive kidney fibrosis. *Kidney Int.* **45**, 916-927 (1994).

23. Ledbetter S., Kurtzberg L., Doyle S., & Pratt B.M. Renal fibrosis in mice treated with human recombinant transforming growth factor-beta2. *Kidney Int.* **58**, 2367-2376 (2000).

24. Moon J.A., Kim H.T., Cho I.S., Sheen Y.Y., & Kim D.K. IN-1130, a novel transforming growth factor-beta type I receptor kinase (ALK5) inhibitor, suppresses renal fibrosis in obstructive nephropathy. *Kidney Int.* **70**, 1234-1243 (2006).

25. Norman J. Fibrosis and progression of autosomal dominant polycystic kidney disease (ADPKD). *Biochim. Biophys. Acta* **1812**, 1327-1336 (2011).

26. Elberg D., Jayaraman S., Turman M.A., & Elberg G. Transforming growth factor-beta inhibits cystogenesis in human autosomal dominant polycystic kidney epithelial cells. *Exp. Cell Res.* **318**, 1508-1516 (2012).

27. Larsson J. *et al.* Abnormal angiogenesis but intact hematopoietic potential in TGF-beta type I receptor-deficient mice. *EMBO J.* **20**, 1663-1673 (2001).

28. Happe H. *et al.* Altered Hippo signalling in polycystic kidney disease. *J. Pathol.* **224**, 133-142 (2011).

29. Moustakas A. & Heldin C.H. The regulation of TGFbeta signal transduction. *Development* **136**, 3699-3714 (2009).

30. Hoogaars W.M. *et al.* Combined effect of AAV-U7-induced dystrophin exon skipping and soluble activin Type IIB receptor in mdx mice. *Hum. Gene Ther.* **23**, 1269-1279 (2012).

31. Leonhard W.N. *et al.* Curcumin inhibits cystogenesis by simultaneous interference of multiple signaling pathways: In vivo evidence from a Pkd1-deletion model. *Am. J. Physiol Renal Physiol* **300**, F1193-F1202 (2011).

32. Happe H. *et al.* Cyst expansion and regression in a mouse model of polycystic kidney disease. *Kidney Int.* **83**, 1099-1108 (2013).

33. Torres V.E. *et al.* Tolvaptan in patients with autosomal dominant polycystic kidney disease. *N. Engl. J. Med.* **367**, 2407-2418 (2012).

34. Caroli A. *et al.* Effect of longacting somatostatin analogue on kidney and cyst growth in autosomal dominant polycystic kidney disease (ALADIN): a randomised, placebo-controlled, multicentre trial. *Lancet* **382**, 1485-1495 (2013).

35. Meijer E. *et al.* Rationale and design of the DIPAK 1 study: a randomized controlled clinical trial assessing the efficacy of lanreotide to Halt disease progression in autosomal dominant polycystic kidney disease. *Am. J. Kidney Dis.* **63**, 446-455 (2014).

36. Lantinga-van Leeuwen I.S. *et al.* Transgenic mice expressing tamoxifen-inducible Cre for somatic gene modification in renal epithelial cells. *Genesis.* **44**, 225-232 (2006).

37. Antsiferova M. & Werner S. The bright and the dark sides of activin in wound healing and cancer. *J. Cell Sci.* **125**, 3929-3937 (2012).

38. Wacker I. *et al.* Key role for activin B in cellular transformation after loss of the von Hippel-Lindau tumor suppressor. *Mol. Cell Biol.* **29**, 1707-1718 (2009).

39. Weimbs T. Regulation of mTOR by polycystin-1: is polycystic kidney disease a case of futile repair? *Cell Cycle* **5**, 2425-2429 (2006).

40. Lee S.J. *et al.* Regulation of muscle growth by multiple ligands signaling through activin type II receptors. *Proc. Natl. Acad. Sci. U. S. A* **102**, 18117-18122 (2005).

41. Sako D. *et al.* Characterization of the ligand binding functionality of the extracellular domain of activin receptor type IIb. *J. Biol. Chem.* **285**, 21037-21048 (2010).

42. Zhou X. *et al.* Reversal of cancer cachexia and muscle wasting by ActRIIB antagonism leads to prolonged survival. *Cell* **142**, 531-543 (2010).

43. Pearsall R.S. *et al.* A soluble activin type IIA receptor induces bone formation and improves skeletal integrity. *Proc. Natl. Acad. Sci. U. S. A* **105**, 7082-7087 (2008).

44. Apostolou E. *et al.* Activin-A overexpression in the murine lung causes pathology that simulates acute respiratory distress syndrome. *Am. J. Respir. Crit Care Med.* **185**, 382-391 (2012).

45. Koncarevic A. *et al.* A novel therapeutic approach to treating obesity through modulation of TGFbeta

signaling. *Endocrinology* **153**, 3133-3146 (2012).

46. Dussiot M. *et al.* An activin receptor IIA ligand trap corrects ineffective erythropoiesis in beta-thalassemia. *Nat. Med.* **20**, 398-407 (2014).

47. Attie K.M. *et al.* A single ascending-dose study of muscle regulator ACE-031 in healthy volunteers. *Muscle Nerve* **47**, 416-423 (2013).

48. Sherman M.L. *et al.* Multiple-dose, safety, pharmacokinetic, and pharmacodynamic study of sotatercept (ActRIIA-IgG1), a novel erythropoietic agent, in healthy postmenopausal women. *J. Clin. Pharmacol.* **53**, 1121-1130 (2013).

49. Hulmi J.J. *et al.* Muscle protein synthesis, mTORC1/MAPK/Hippo signaling, and capillary density are altered by blocking of myostatin and activins. *Am. J. Physiol Endocrinol. Metab* **304**, E41-E50 (2013).

50. Ruijter J.M. *et al.* Amplification efficiency: linking baseline and bias in the analysis of quantitative PCR data. *Nucleic Acids Res.* **37**, e45 (2009).

51. Persson U. *et al.* The L45 loop in type I receptors for TGF-beta family members is a critical determinant in specifying Smad isoform activation. *FEBS Lett.* **434**, 83-87 (1998).

Supplemental Figure 1. Effect of sActRIIB-Fc on renal histology in Pkd1-cKO mice.

Each litter was subdivided in a PBS, 3 mg/kg, or 10 mg/kg sActRIIB-Fc treatment group. Histology of all mice are shown. M; indicates male, F; indicates female. The mice on sActRIIB-Fc treatment had improved renal histology compared to the PBS treated mice.

SUPPLEMENTAL FIGURES

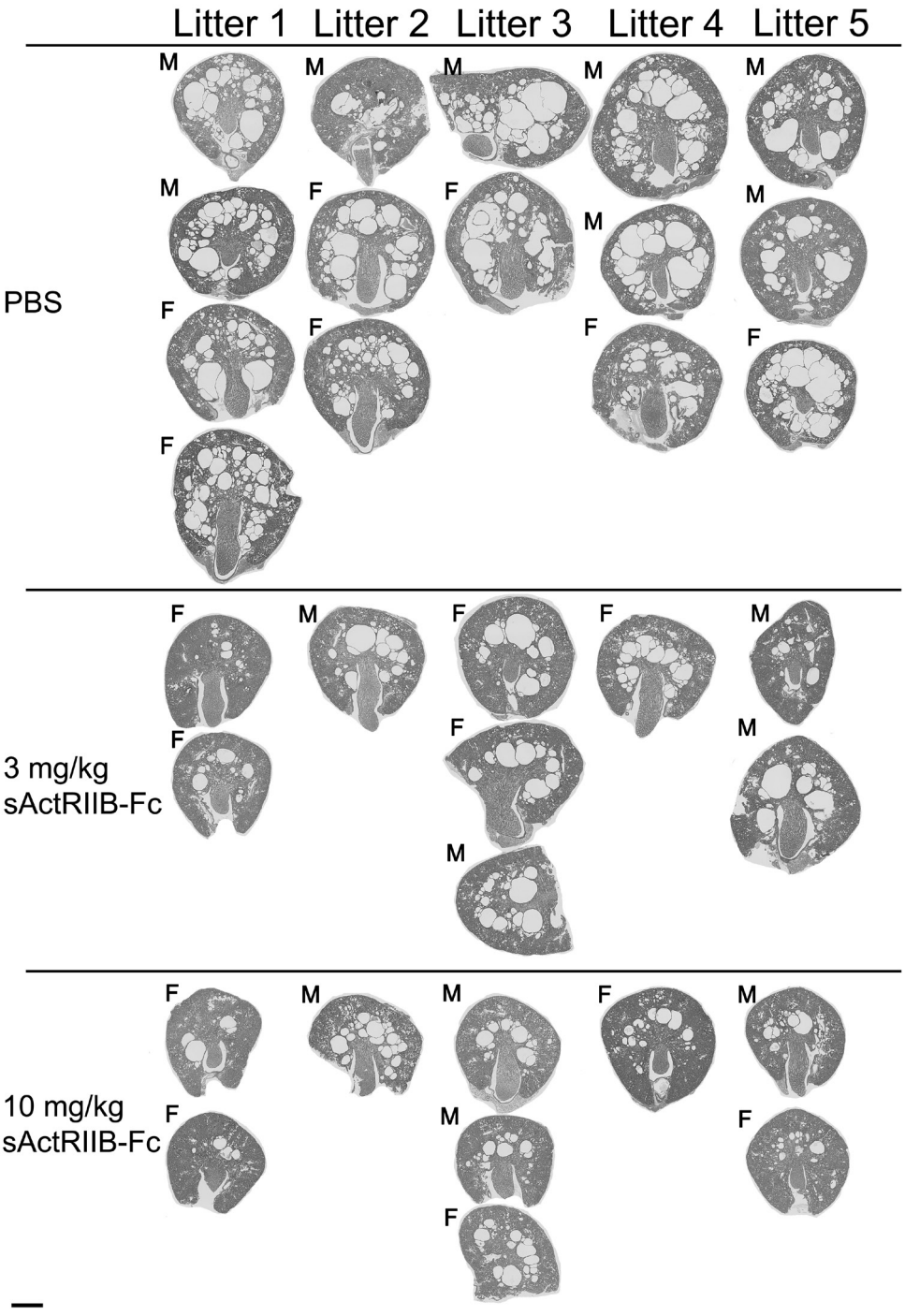

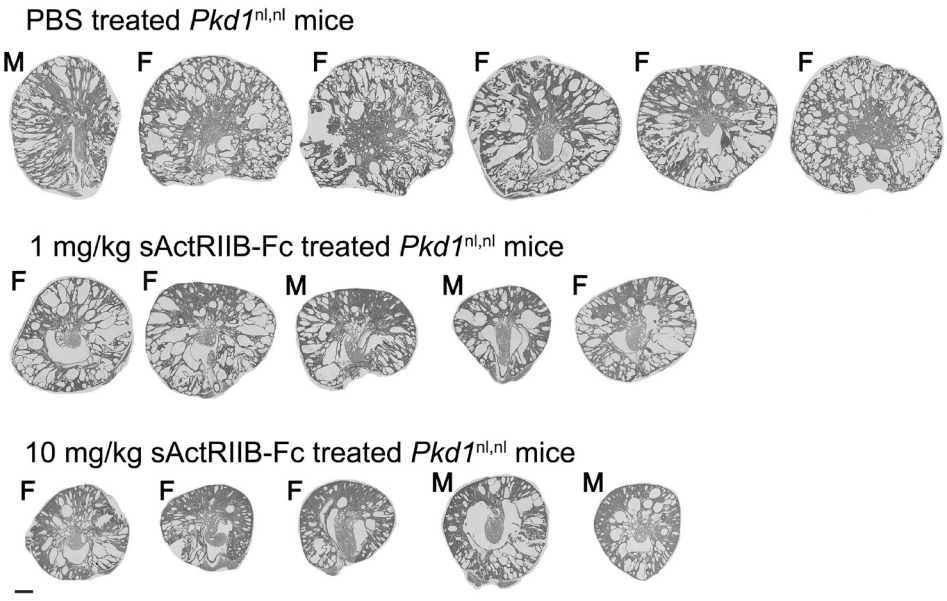

Supplemental Figure 2. Effect of sActRIIB-Fc on renal histology in Pkd1^{nl,nl} mice.

The mice were treated 4 times between P10-P21 with either PBS alone, 1 mg/kg, or 10 mg/kg sActRIIB-Fc. Renal histology of all mice are shown. M; indicates male, F; indicates female. The kidneys from mice on sActRIIB-Fc were smaller and generally appeared less cystic compared to the kidneys of the PBS treated mice. Scale bar: 1 mm

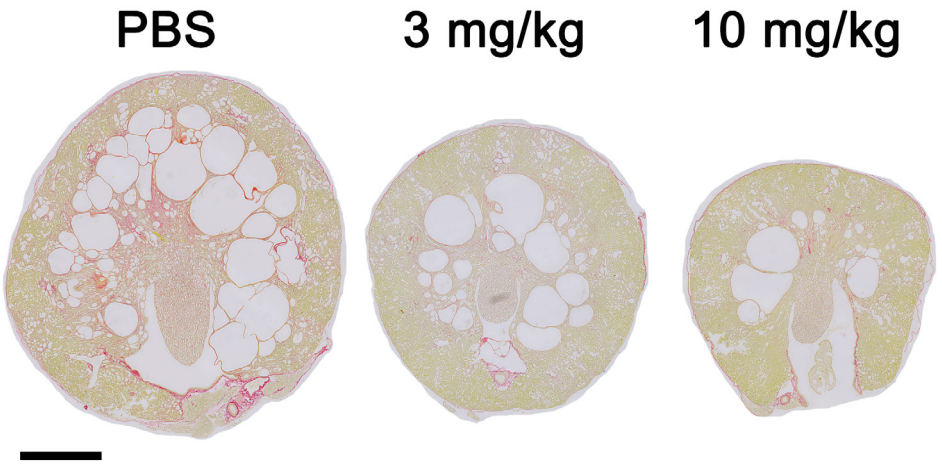

Supplemental Figure 3. Example images of SiriusRed stainings of renal sections of P10-*Pkd1*-cKO mice that were either treated with PBS, 3 mg/kg or 10 mg/kg sActRIIB-Fc. Quantification is shown in Figure 5C.

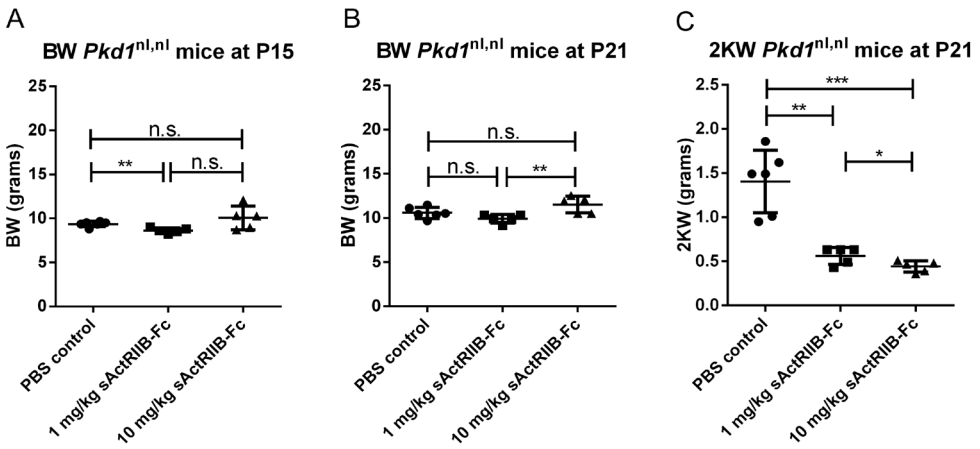

Supplemental Figure 4. Characteristics of the P18-*Pkd1*-cKO mouse model.

Pkd1-cKO mice were treated with 150 mg/kg Tamoxifen or left untreated. At 4 weeks after Tamoxifen (*n* = 9 mice), the 2KW/BW% had increased slightly compared to control mice without Tamoxifen (*n* = 12 mice). The mice were then followed until the onset of renal failure (indicated as having a BU > 20 mmol/L; *n* = 6 mice), which occurred approximately at 100 days of age (see also Figure 6), with 2KW/BW% of approximately 8%. Segmental marker staining using anti-Megalin (proximal tubular marker), anti-Tammhorsfall protein (distal tubular marker), or Anti-Aqp2 antibodies (Collecting duct marker), revealed cyst formation from all tubular segments. Differences in 2KW/BW% between all groups: *** $P < 0.001$

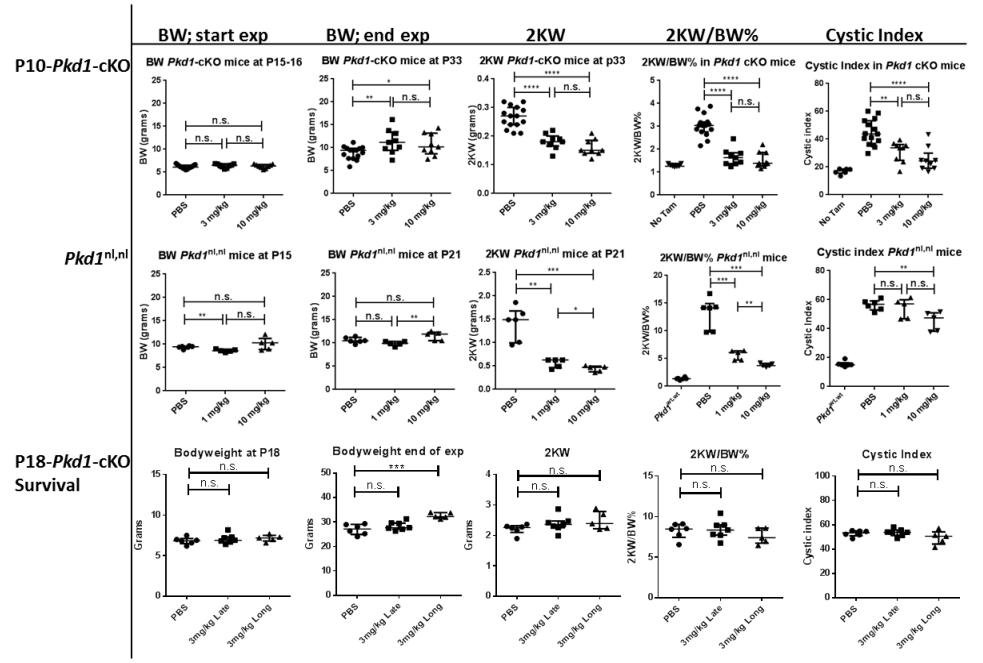

Supplemental Figure 5. Summary of bodyweight (BW) and total kidney weights (2KW).

Summary of bodyweight (BW) at the beginning and at the end of the experiment, of the total kidney weights (2KW) and of the 2KW/BW%, and of the cystic indices of all mice in this study is shown. Of note, the sActRIIB-Fc treated mice that were euthanized at fixed time points (the P10-*Pkd1*-cKO and the *Pkd1*^{nl,nl} mice) had lower kidney weights and lower cystic indices compared to their PBS treated littermates. The kidney weights and cystic indices were not different between the groups of the P18-*Pkd1*-cKO mice but the progression was slower in the sActRIIB-Fc treated mice compared to their PBS treated littermates (see Figure 6). * indicates $P < 0.05$, ** indicates $P < 0.01$, *** indicates $P < 0.001$, **** indicates $P < 0.0001$.). n.s. indicates Not significant

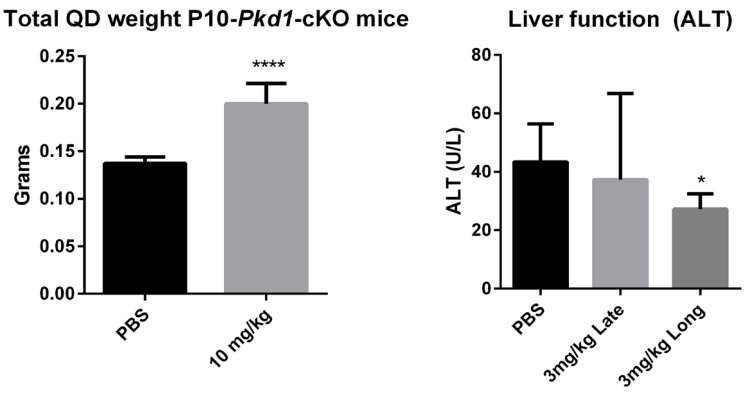

Supplemental Figure 6. Additional effects of sActRIIB-Fc.

The weight of the quadriceps's (QD) of sActRIIB-Fc treated P10-*Pkd1*-cKO mice (10 mg/kg) is higher than the QD weight of their PBS treated littermates. Alanine aminotransferase (ALT) blood levels were measured in the P18-*Pkd1*-cKO mice at the end of the experiment. Liver function was normal in all tested groups. * indicates $P < 0.05$, **** indicates $P < 0.0001$.

SUPPLEMENTARY MATERIALS CAN BE DOWNLOADED FROM

https://goo.gl/693ao1